A FAK scaffold inhibitor disrupts FAK and VEGFR-3 signaling and blocks melanoma growth by targeting both tumor and endothelial cells

Elena Kurenova[1,6], Deniz Ucar[5], Jianqun Liao[1], Michael Yemma[1], Gogate Priyanka[1], Wiam Bshara[2] , Ulas Sunar[3], Mukund Seshadri[4], Steven N. Hochwald[1] and William G. Cance[1,6] .

Supplementary Materials and Methods

Development of fluorescence polarization (FP)-based binding assays for FAK protein

Sensitive and quantitative FP-based binding assay was developed to determine the binding affinity of FAK scaffold inhibitors to the recombinant FAK protein using the Perkin Elmer EnVision 2103 Multilabel Reader and software Wallac Envision Manager 1.12.

Determine Kd value of TAMRA probe to protein

The 12-mer VEGFR-3 derived peptide AV3 (1) was 5-carboxytetramethylrhodamine (TAMRA)-conjugated (Biomatik, Wilmington, DE) and used as the fluorescent probe in the FP-based binding assays (TAMRA- Acp-WHWRPWTPCKMF-NH_2). The corresponding unlabeled peptide AV3 (Biomatik, Wilmington, DE) was used in the competition assay. The Kd value was determined to FAK protein with a fixed concentration of the tracer (175 nM of AV3-TAMRA) and increasing concentrations (0.97 µM - 200 µM) of FAT domain protein, in a final volume of 125 µl in the assay buffer (5 mM dithiothreitol (DTT), 0.05% BSA, and 0.05% Triton X-100 in PBS at pH 6.5). Plates (384 well non-binding surface flat bottom black well plates, Corning) were mixed and incubated at room temperature for 1 hour and the polarization values in millipolarization units (mP) were measured at an excitation wavelength of 531 nm and an emission wavelength of 579 nm.

Equilibrium dissociation constants (Kd) were calculated by using the non-linear curve fitting algorithms of Graphpad Prism 6.0 software (Graphpad Software).

Determine IC_{50} values of FAK scaffold inhibitors

Based on the Kd values, the concentrations of the FAT protein used in the competitive binding experiments was 40 µM. The fluorescent probe AV3-TAMRA were fixed at 175 nM for all assays. A range of concentrations of unlabeled AV3 (0.39 µM – 200 µM), C4 (0.97 µM – 250 µM), and C1 (0.97 µM – 250 µM) were used for competition assays. 100 µL of protein/probe complex in the assay buffer (5 mM dithiothreitol (DTT), 0.05% BSA, and 0.05% Triton X-100 in PBS at pH 6.5) were added to assay plates

(384 well non-binding surface flat bottom black well plates, Corning), incubated at room temperature for 1 h and the polarization values (mP) were measured at an excitation wavelength of 531 nm and an emission wavelength of 579 nm. Non-linear curve fitting algorithms were used to calculate the inhibition constants (one site log IC_{50}) using GraphPad Prism 6.

Antibodies and reagents

VEGFR-3 and p-VEGFR-3 rabbit polyclonal antibody from Cell Aplications, Inc. and Santa Cruz Biotechnology, Inc. (Santa Cruz, CA, USA). Cell Signaling Technology (Danvers, MA, USA): Pro-caspase-8, -3; PARP.

Apoptosis assay

After treatment of cells for 24, 48, and 72 hours cells were collected, counted and prepared for terminal uridine deoxynucleotidyl transferase (TUNEL) assay by utilizing an APO-BRDU kit (BD Pharmingen, San Diego, CA) according to the manufacturer's instructions. Stained cells were analyzed with a FACSCalibur cytometer (Becton Dickinson, San Jose, CA). Calculation of the percentage of apoptotic cells in the sample was completed with CellQuest software (BD Biosciences).

Motility wound healing assay

For the measurement of cell migration during wound healing, human C8161 cells were seeded on 24-well plates. Confluent cell cultures were incubated in serum-free medium for 24 h and were wounded by scraping with a 100-µL pipette tip, washed to remove debris and incubated in medium containing 10% FBS with or without C4 (10 and 50 µM), as indicated. Cells were photographed after wounding by phase contrast microscopy (Axiovert200, Zeiss) at 12, 24 and 48 h. Experiments were done in duplicate and two fields of each well were recorded. Image analysis was done with WimScratch module of Wimasis software.

Magnetic Resonance Imaging

MRI examinations were performed in mice bearing C8161 melanoma xenografts with matched tumor volumes (n = 3 per group). Experimental MRI examinations were carried out in a 4.7 T/33-cm horizontal bore magnet (GE NMR Instruments, Fremont, CA) incorporating AVANCE digital electronics

(Bruker Biospec with ParaVision 3.0.2; Bruker Medical Inc., Billerica, MA) and a removable gradient coil insert (G060, Bruker Medical Inc., Billerica, MA) generating maximum field strength of 950 mT/m and a custom-designed 35-mm RF transmit-receive coil. Mice were placed on a form-fitted MR-compatible sled (Dazai Research Instruments, Toronto, Canada) and supplied with 2% isoflurane during image acquisition. Respiration rates and core-body temperature were monitored continuously while mice were in the scanner. Preliminary scout images were acquired on the sagittal and axial planes to assist in slice prescription for subsequent scans. Multislice non contrast-enhanced T2-weighted images were acquired on the axial planes with the following parameters: TE_{eff} = 41 ms, TR = 2500 ms, FOV = 3.2 x 3.2 cm, matrix size = 256 x 192, 25 slices, slice thickness 1 mm). T1-weighted (T1W) contrast-enhanced MRI was performed using albumin-gadopentetate dimeglumine (albumin-GdDTPA) as described previously (2-4). A series of eight T1-weighted images (3 precontrast and 5 post contrast) were acquired over ~45 minutes. Albumin-Gd-DTPA was administered at a dose of 0.05 mmol/kg as a bolus *via* tail-vein injection after completion of 3 baseline precontrast images. The vascular relaxation enhancement after administration of albumin-GdDTPA was measured using a balanced steady state precession, inversion recovery technique (TrueFISP) as described previously (3). Raw image datasets were transferred to a workstation for post processing using AnalyzeTM (AnalyzeDirect, Overland Park, KS) and MATLAB (Version 7.0, Mathworks Inc., Natick, MA). Regions of interest (ROI) were manually defined for the entire tumor, blood vessel, kidneys and murine muscle tissues at each time point. At least 2–3 slices were evaluated for each tumor. The change in R1 (ΔR1) following contrast agent injection was assumed to be proportional to the tissue concentration of the contrast agent. Blood R1 curves were fitted to monoexponential decay. Kinetic analysis of ΔR1tumor (normalized to the fit values of ΔR1 in blood) was performed to estimate the fractional blood volume (BV; y-intercept) (2, 3). Relative blood volume maps were calculated on a pixel-by-pixel basis using MATLAB (Version 7.0, Mathworks Inc., Natick, MA) and pseudo-colorized in Analyze™.

Diffuse Correlation Spectroscopy for Blood Flow Quantification

Tissue blood flow was measured using a previously described and validated diffuse correlation spectroscopy (DCS) instrument (5, 6), which measures rapid light intensity temporal fluctuations in tissue and then uses the autocorrelation functions associated with these fluctuations to extract information about the speed of moving tissue scatterers, in this case red blood cells (7). The decay rate of the autocorrelation

function is related to blood flow (8). Optical blood flow measurements were performed with a system comprised of three main components: a long coherence length laser operating at 785 nm, a photon-counting detector, and a custom built autocorrelator board. The optical probe contained one multimode laser source fiber and four single-mode detector fibers so that four source-detector separations ranging from 2mm to 4mm were obtained. For each measurement, the four detector signals were averaged to obtain average blood flow. Skeletal muscle away from the tumor was measured for comparison. Five independent measurements were performed by placing the optical probe at slightly different spatial positions. Photodetector outputs were fed into a correlator board, and intensity autocorrelation functions and photon arrival times were recorded by a computer for further processing to extract blood-flow-related parameters. We generally report relative blood flow, rBF, to describe blood flow changes during therapy: rBF is a blood flow parameter measured relative to its pre-treatment value. Blood flow was measured before treatment to obtain baseline levels and subsequent measurements were performed 7 days and 14 days after treatment. Measurements were normalized to baseline values to quantify changes in relative blood flow due to C4 treatment.

Supplementary Figures.

Supplementary Figure S1. FAK scaffold inhibitor C4 reduced phosphorylation of VEGFR-3 and decreased FAK-VEGFR3 complex formation. C4 dose-dependent decrease of FAK-VEGFR-3 association in melanoma C8161 cells. Cells were treated with increased concentrations C4 for 24 h. A. VEGFR-3 protein complexes were immunoprecipitated (IP) with VEGFR-3 antibody (Millipore, clone 9D9) and precipitates were analyzed in consequent western blotting (WB) for VEGFR-3 phosphorylation with pan-phospho-tyrosine antibody 4G10 (P-Tyr) and for the presence of FAK protein with FAK specific antibody (Millipore, clone 4.47). B. Densitometry was performed for each IP experiment and data are presented at the bottom of the western blot image. Left panel - decrease of P-Tyr phosphorylation of VEGFR-3; right panel - decrease of FAK protein in VEGFR-3 co-precipitates.

Supplementary figure S2. **FAK scaffold inhibitor C4 inhibited motility of melanoma cells.** A. The wound healing assay of C4 treated C8161 cells. Image analysis was done with WimScratch module of Wimasis software. Data shown are representative of three independent experiments. B. Graphical

representation of the quantitative values of the wound size at different doses and at different time points post-C4 treatment. The error bar represents ±SEM.

Supplementary figure S3. FAK scaffold inhibitor C4 caused apoptosis in melanoma cell lines. C8161 and A375 cells were treated with increased concentration of C4 for 48 h and 72 h and percentage of TUNEL positive cells were determined by FACS. STS – staurosporin was used as a positive control.

Supplementary figure S4. FAK scaffold inhibitor C4 sensitized melanoma cells to cytotoxic therapy and caused apoptosis in melanoma cell lines. Western blot analysis of biochemical markers of the apoptotic pathway. A. C8161 cells were treated for 48 h with 60 μM of C4 and 10 μM DTIC alone or in combination and activation of Caspase 8, Caspase 3 and PARP cleavage are analyzed. B. A375 cells were treated for 48 h with 60 μM of C4 and 20 μM DTIC alone or in combination. All shown figures are representative of experiments performed in triplicate.

Supplementary figure S5. **FAK scaffold inhibitor C4 inhibited tumor growth *in vivo*.** A. Mice weight, IP treatment with PBS or C4 50 mg/kg for 62 days. B. Mice weight in PBS and C4 50 mg/kg treatment groups at the end of the experiment at day 62. C. Heart, lung, liver, spleen, kidney weight in PBS and C4 50 mg/kg treatment groups at the end of the experiment at day 62. D. Panel represents mean C8161 tumor weight ±SEM at the end of the experiment at day 23. Female nude mice were subcutaneously inoculated with C8161 cancer cells (5 mice/ group). IP with compound C4 (25mg/kg, daily), DTIC (8 mg/kg, Q4D) and combination were started when tumor reach 100 mm^3. * $P<0.05$ and ** $P<0.01$ relative to untreated control, @ relative to C4 alone, # relative to chemotherapy alone. E. Panel represents mean A375 tumor weight ±SEM at the end of the experiment at day 31. Female nude mice were subcutaneously inoculated with melanoma A375 cells (5 mice/group). IP with compound C4 (25mg/kg, daily), DTIC (8 mg/kg, Q4D) and combination were started when tumor reached 100 mm^3 and continued for 31 days.

REFERENSES

1. Garces CA, Kurenova EV, Golubovskaya VM, Cance WG. Vascular endothelial growth factor receptor-3 and focal adhesion kinase bind and suppress apoptosis in breast cancer cells. Cancer Res. 2006;66:1446-54.
2. Seshadri M, Mazurchuk R, Spernyak JA, Bhattacharya A, Rustum YM, Bellnier DA. Activity of the vascular-disrupting agent 5,6-dimethylxanthenone-4-acetic acid against human head and neck carcinoma xenografts. Neoplasia. 2006;8:534-42.

3. Seshadri M, Merzianu M, Tang H, Rigual NR, Sullivan M, Loree TR, et al. Establishment and characterization of patient tumor-derived head and neck squamous cell carcinoma xenografts. Cancer Biol Ther. 2009;8:2275-83.
4. Seshadri M, Sacadura N, Coulthard T. Monitoring antivascular therapy in head and neck cancer xenografts using contrast-enhanced MR and US imaging. Angiogenesis. 2011;14:491-501.
5. Rohrbach DJ, Rigual N, Tracy E, Kowalczewski A, Keymel KL, Cooper MT, et al. Interlesion differences in the local photodynamic therapy response of oral cavity lesions assessed by diffuse optical spectroscopies. Biomedical optics express. 2012;3:2142-53.
6. Sunar U, Rohrbach D, Rigual N, Tracy E, Keymel K, Cooper MT, et al. Monitoring photobleaching and hemodynamic responses to HPPH-mediated photodynamic therapy of head and neck cancer: a case report. Opt Express. 2010;18:14969-78.
7. Boas DA, Campbell LE, Yodh AG. Scattering and Imaging with Diffusing Temporal Field Correlations. Phys Rev Lett. 1995;75:1855-8.
8. Mesquita RC, Durduran T, Yu G, Buckley EM, Kim MN, Zhou C, et al. Direct measurement of tissue blood flow and metabolism with diffuse optics. Philosophical transactions Series A, Mathematical, physical, and engineering sciences. 2011;369:4390-406.

Supplementary Figure S1

A

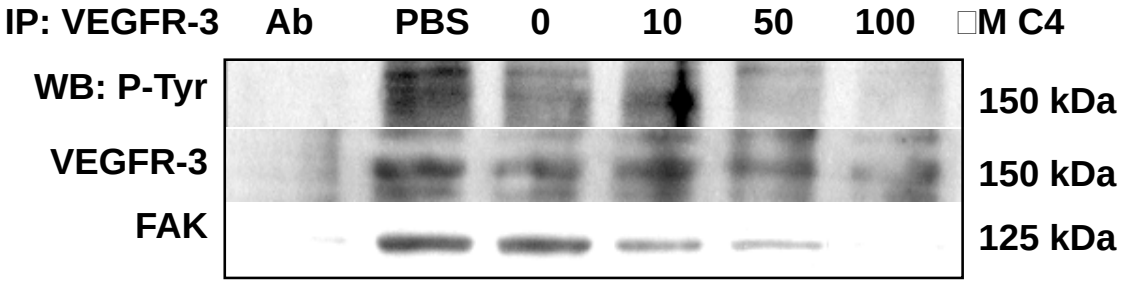

B

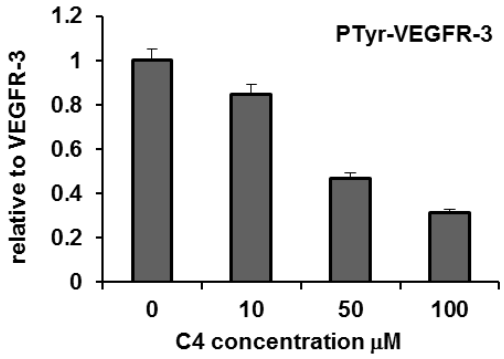

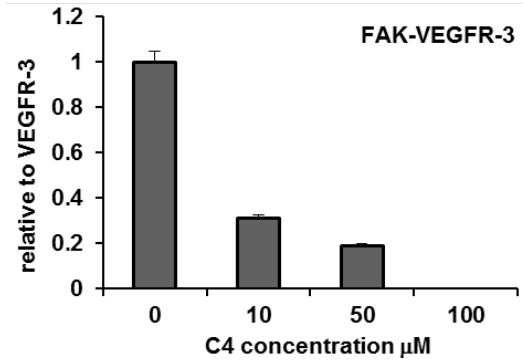

Supplementary Figure S2

A

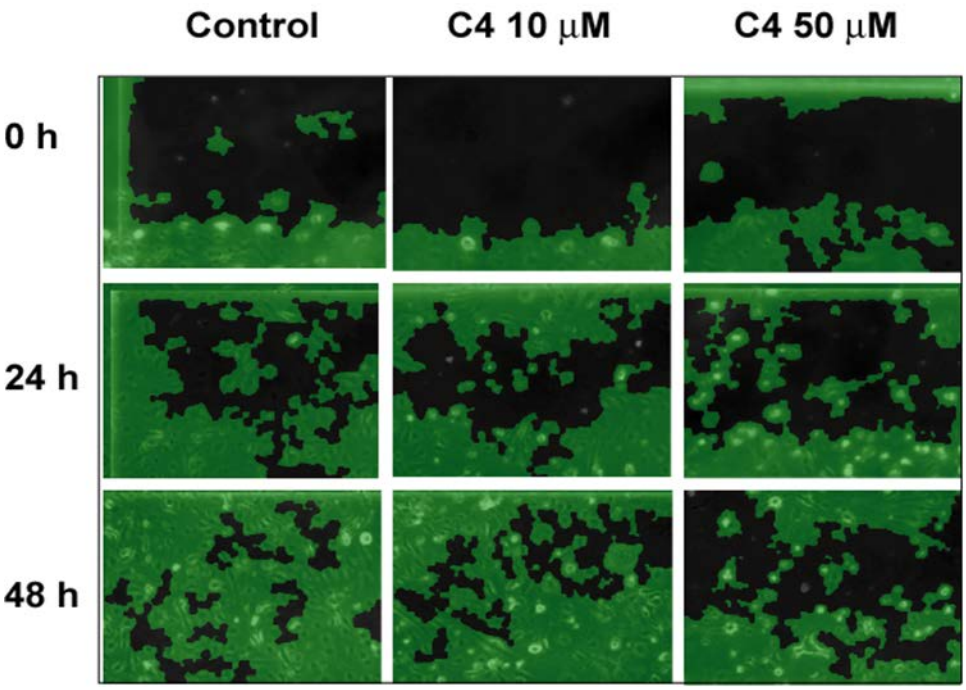

B

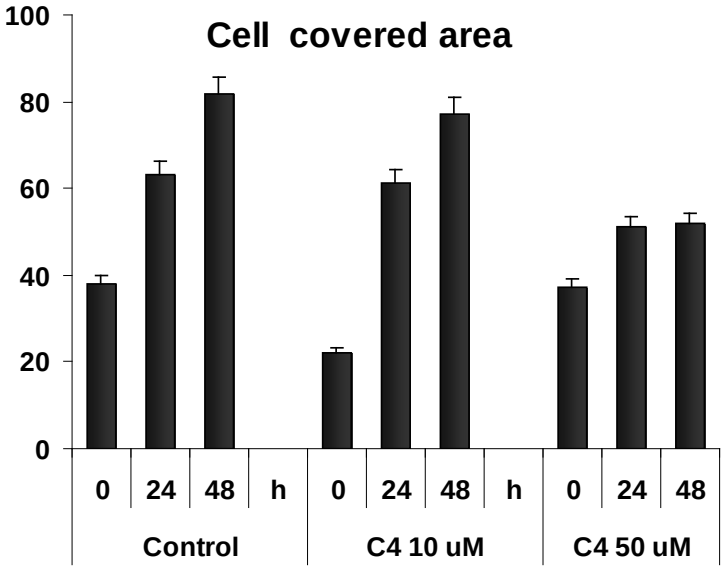

Supplementary Figure S3

A

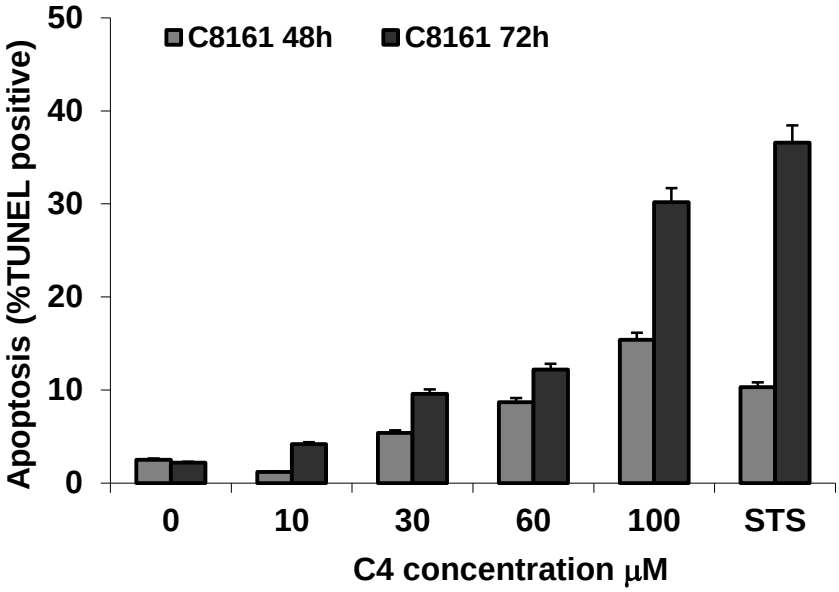

B

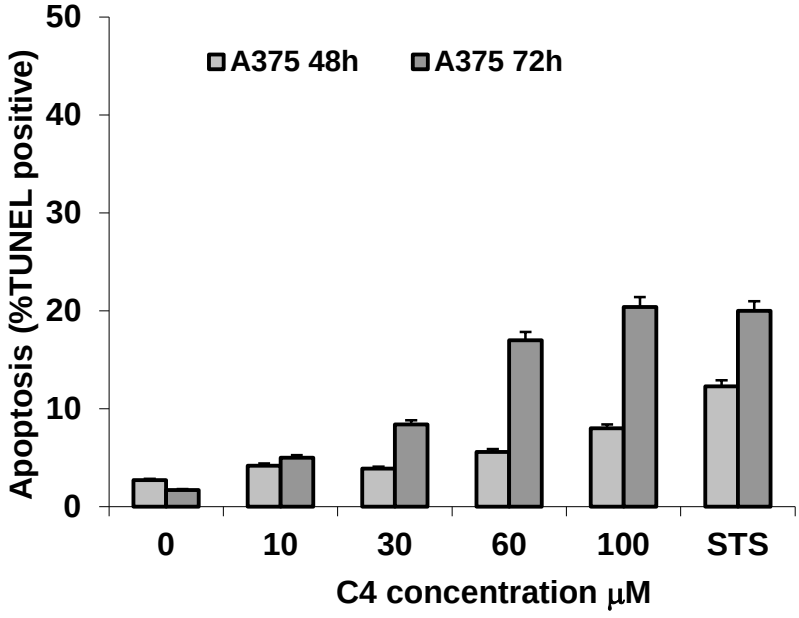

A

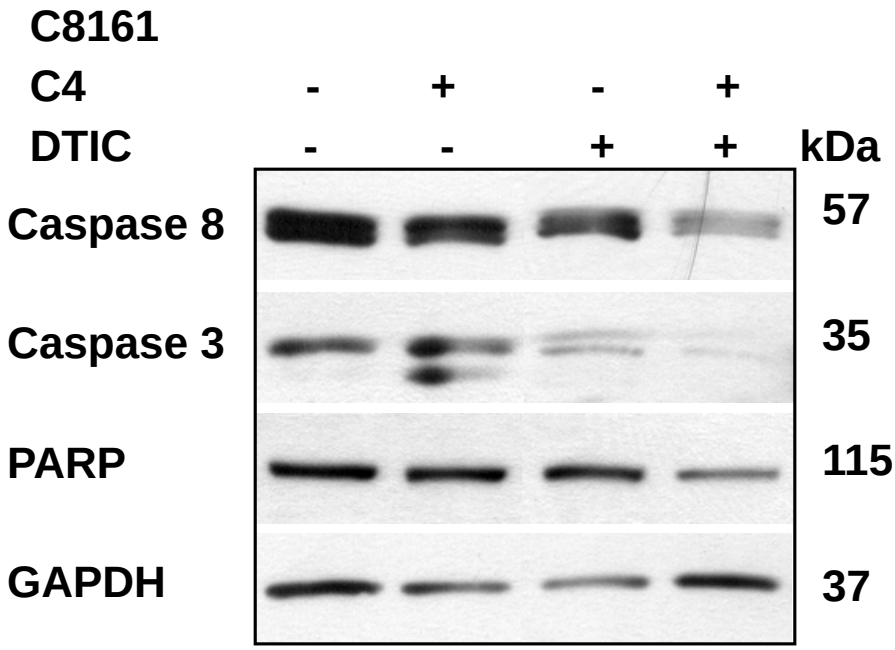
C8161
C4 - + - +
DTIC - - + +
kDa
Caspase 8
57
Caspase 3
35
PARP
115
GAPDH
37

B

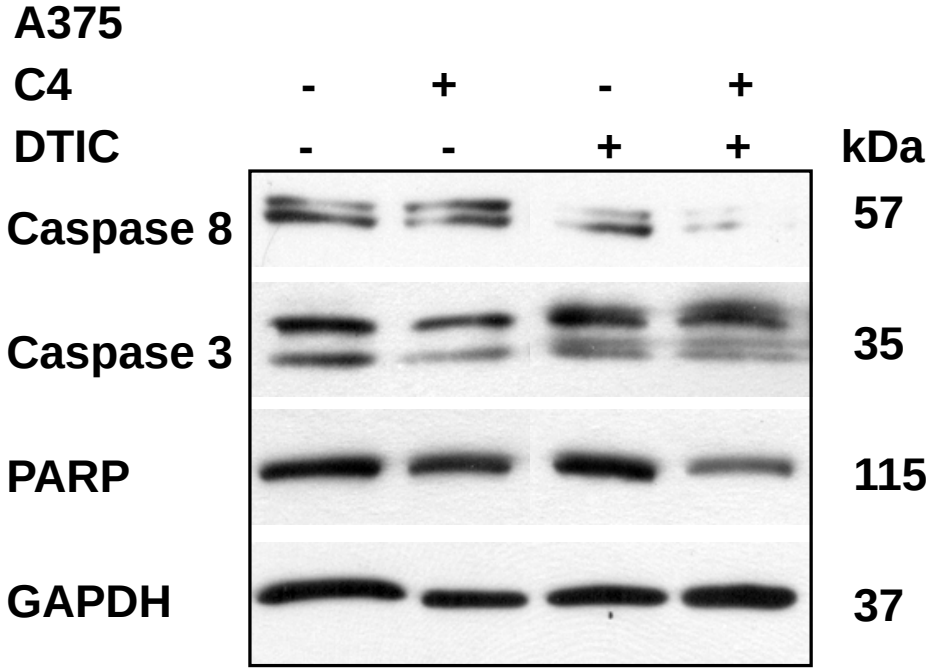
A375
C4 - + - +
DTIC - - + +
kDa
Caspase 8
57
Caspase 3
35
PARP
115
GAPDH
37

Supplementary Figure S5

A

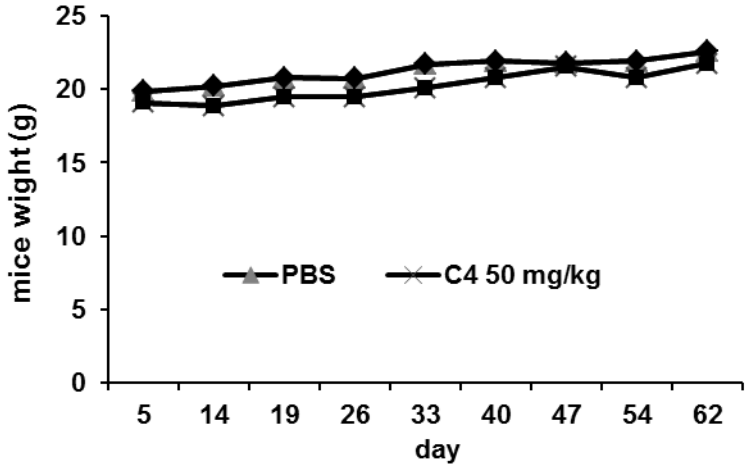

B

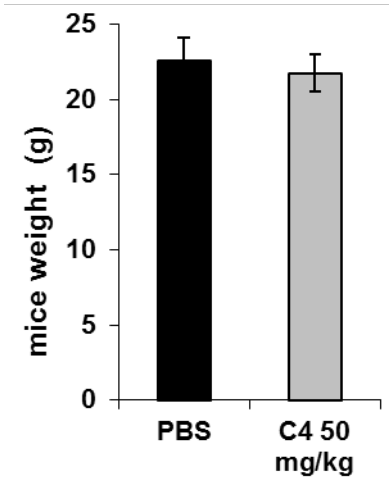

C

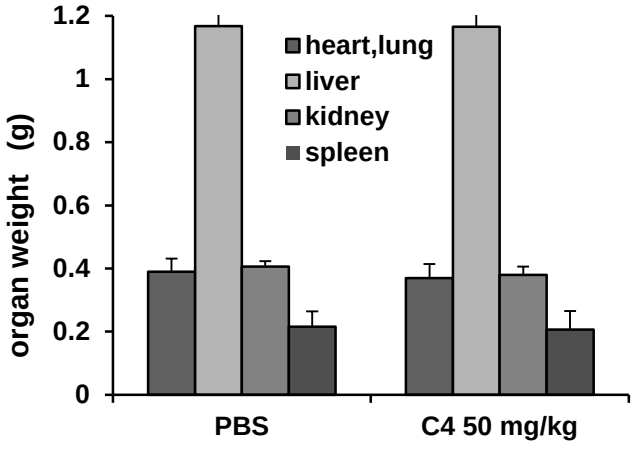

D

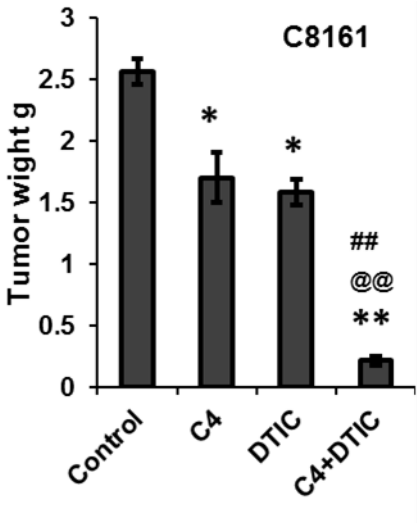

E